npg

Original Article

The role of TRPC6 in HGF-induced cell proliferation of human prostate cancer DU145 and PC3 cells

Yong Wang[1], Dan Yue[2], Kai Li[3], Yi-Li Liu[1], Chang-Shan Ren[4], Ping Wang[1]

[1]Department of Urology, Fourth Affiliated Hospital, China Medical University, Shenyang 110032, China
[2]College of Medical Laboratory Science, Tianjin Medical University, Tianjin 300070, China
[3]Department of Surgical Oncology, First Affiliated Hospital, China Medical University, Shenyang 110001, China
[4]Cancer Research Institute, First Affiliated Hospital, China Medical University, Shenyang 110001, China

Abstract

Hepatocyte growth factor (HGF) is a glycoprotein that induces prostate cancer cell proliferation, migration and invasion. The activation of transient receptor potential canonical 6 (TRPC6) channels is considered important in promoting prostate cancer cell proliferation. In this study, we assessed the role of endogenous TRPC6 channels in the HGF-induced cell proliferation of prostate cancer. Reverse transcription-PCR and Western blotting were used to investigate TRPC6 expression. Electrophysiological techniques (whole-cell patch clamp configuration) and Ca^{2+} imaging analysis were used to investigate the channel activity in cells. The effects of TRPC6 channels on cell cycle progression, cell apoptosis and cell growth were also examined. TRPC6 and c-MET were expressed in DU145 and PC3 cells. In addition, functional TRPC6 channels were present in DU145 and PC3 cells, and TRPC6 knockdown suppressed TRPC-like currents evoked by oleoyl-2-acetyl-sn-glycerol (OAG). Inhibition of TRPC6 channels in DU145 and PC3 cells abolished OAG- and HGF-induced Ca^{2+} entry. Furthermore, inhibition of TRPC6 channels arrested DU145 and PC3 cells at the G_2/M phase and suppressed HGF-induced cell proliferation. Collectively, our results indicate that TRPC6 has an important role in HGF-induced DU145 and PC3 cell proliferation.

1 Introduction

Prostate cancer, a common malignant tumour, is now the second leading cause of cancer-related deaths of men in Western societies. After metastasis to bone and lymph nodes, the primary cause of prostate cancer mortality is the progression from androgen-dependent to androgen-independent growth. After androgen escape, prostate cancer cell proliferation becomes independent of normal growth control mechanisms, and no effective therapy for this proliferation is currently available [1]. Ion channels have critical roles in tumour development. As a result, K^+ and Na^+ channels are being developed as targets for cancer therapy [2]. Ca^{2+} signalling is also regarded as important for cell proliferation [3], cell cycle transition [4] and cell apoptosis [5].

Transient receptor potential (TRP) channels are a large family of non-selective cation channels and were initially characterized as light sensors in the photoreceptors of *Drosophila* [6]. TRP canonical (TRPC) channels, a subfamily of TRP channels in mammalian

cells, include seven members (TRPC1–7) and are mostly permeable to Ca^{2+}. Through a phospholipase C (PLC)-dependent mechanism, they can be activated by G-protein coupled receptors or receptor tyrosine kinases [7]. Recently, it has been shown that TRPC6 contributes to the proliferation of some types of cancer cells [8–10]. In addition, in the primary human prostate cancer epithelial (hPCE) cells and LNCaP cells, agonist-mediated stimulation of α_1-adrenergic receptors requires the coupled activation of TRPC6 channels and nuclear factors of activated T cells to promote cell proliferation [11, 12].

A higher plasma level of hepatocyte growth factor (HGF) in prostate cancer patients is associated with an advanced stage of malignancy and a poor prognosis [13, 14]. HGF stimulates cell proliferation, migration and invasion, at least in part, through HGF-receptor-mediated calcium influx. HGF-induced Ca^{2+} oscillations are observed in hepatocytes [15]. HGF induces epithelial tubular cell proliferation, migration, scattering and tubulogenesis through KCNA1, TRPC6 and NHE1 [16]. In addition, El Boustany *et al.* [9] found that endothelial growth factor (EGF) and HGF increase TRPC6 levels and induce a large increase in store-operated calcium entry amplitude in Huh-7 cells. However, the mechanisms by which HGF induces this calcium entry are not yet understood.

Our previous experiments have shown that TRPC6 expression is associated with tumour grade in prostate cancer [17] and that HGF induces DU145 cell proliferation, migration and invasion [18]. On the basis of these observations, we examined whether TRPC6 has a role in HGF-induced proliferation of prostate cancer cells using electrophysiological and molecular techniques.

2 Materials and methods

2.1 Cell culture

The LNCaP, 22Rv1, DU145 and PC3 prostate cancer cell lines were obtained from American Type Culture Collection (ATCC, Rockville, MD, USA). The PC3 cells were maintained in DMEM/F12 (GIBCO BRL, Gaithersburg, MD, USA) and the LNCaP, DU145 and 22Rv1 cells were cultured in RPMI 1640 (GIBCO BRL). They were all supplemented with 10% (v/v) fetal calf serum (Invitrogen, Carlsbad, CA, USA) and incubated at 37ºC with 5% CO_2.

2.2 Reverse transcription-Polymerase Chain Reaction analysis (RT-PCR)

Total RNA was isolated from cells using the Trizol reagent (Invitrogen). The RNA (500 ng) was then reverse-transcribed into cDNA using oligo (dT) primers and AMV Reverse Transcriptase (Takara, Shiga, Japan). Next, 10 μL of cDNA was used for PCR in a final reaction volume of 50 μL. For PCR, specific sense and antisense primers were selected. The human *TRPC6* primers (NM_004621) were as follows: sense 5′-GAACTTAGCAATGAACTGGCAGT-3′ and antisense 5′-CATATCATGCCTATTACCCAGGA-3′, with a product length 625 bp for *TRPC6* and 277 bp for *TRPC6γ* [12]. The human *c-MET* primers (NM_000245) were as follows: sense 5′-GTTTCCCAATTTCTGACC-3′ and antisense 5′-TATATCAAAGGTGTTTAC-3′, with a product length of 516 bp. The *β-actin* primers (NM_001101) were as follows: sense 5′-TGGGCATGGGTCAGAAGGAT-3′ and antisense 5′-AAGCATTTGCGGTGGACGAT-3′, with a product length of 991 bp. Primers were synthesized by Takara. DNA amplification conditions included an initial 5 min denaturation step at 95ºC and 30 cycles of 30 s at 95ºC, 30 s at 58ºC (*TRPC6* and *β-actin*) or 60ºC (*c-MET*) and 40 s at 72ºC, followed by a final elongation of 7 min at 72ºC. The RT-PCR samples were electrophoresed on a 1.5% agarose gel and stained with ethidium bromide (0.5 μg mL^{-1}); the gels were then photographed under ultraviolet transillumination.

2.3 Western blotting

Total proteins from prostate cancer cells were extracted. Equal amounts of each protein sample (80 μg) were separated by SDS-polyacrylamide gel electrophoresis and transferred onto polyvinylidene fluoride membranes (Invitrogen) using a wet transfer. Immunoblotting was performed with a rabbit polyclonal primary anti-TRPC6 antibody (diluted 1:500, Abcam, Cambridge, UK), a primary rabbit anti-human c-MET polyclonal antibody (diluted 1:50, Thermo Fisher Scientific, Cheshire, UK) or a goat polyclonal primary anti-β-actin (diluted 1:1 000, Santa Cruz, CA, USA) and then developed with the enhanced chemiluminescence system (Amersham, Uppsala, Sweden) using specific peroxidase-conjugated anti-IgG secondary antibodies. The bands were quantified by densitometry using ImageJ software (NIH, Bethesda, MD, USA), and the values are shown as ratios.

2.4 Silencing of TRPC6

Transfection was accomplished using the follow-

ing target sequences for *TRPC6* (siRNA1: sense, 5′-GGAAGCAAUUCTCAGUCAUTT-3′; antisense, 5′-AUGACUGAGAAUUGCUUCCTT-3′. siRNA2: sense, 5′-GCUUACCUGUCAUUGUCUAUTT-3′; antisense, 5′-UAGACAAUGACAGGUAAGCTT-3′. siRNA control: sense, 5′-UUCUCCGAACGUGUCACGUTT-3′; antisense, 5′-ACGUGACACGUUCGGAGAATT-3′). Briefly, 24-well plates were seeded at 2.5 × 10^4 cells per well 24 h before transfection. Transfection mixes were set-up with diluted siRNA (40 pmol of siRNA in 50 μL of Optimem) and diluted lipofectamine (1.5 μL of lipofectamine in 50 μL of Optimem) (total volume = 100 μL per well). Transfection mixes were applied to the cells for 5 h before being removed and replaced with 1 mL of growth medium.

2.5 Electrophysiology

For the electrophysiological analysis, cells grown on glass coverslips were transferred to the recording chamber and maintained in a standard external solution (145 mmol L^{-1} NaCl, 5.4 mmol L^{-1} KCl, 1 mmol L^{-1} MgCl$_2$, 2 mmol L^{-1} CaCl$_2$, 10 mmol L^{-1} HEPES and 10 mmol L^{-1} glucose, adjusted with NaOH to pH 7.4). Currents were recorded in voltage-clamp mode, using a MultiClamp 700B (Axon Instruments, Foster City, CA, USA). PClamp 8.0 software (Axon Instruments) was used to control the voltage, as well as to acquire and analyse the data. An Ag–AgCl wire was used as a reference electrode. Borosilicate fire-polished pipettes had resistances between 3 and 5 MΩ after being filled with the standard pipette solution (140 mmol L^{-1} CsCl, 5 mmol L^{-1} CaCl$_2$, 1 mmol L^{-1} ATP-Na$_2$, 10 mmol L^{-1} HEPES, 10 mmol L^{-1} EGTA, 2 mmol L^{-1} MgCl$_2$, adjusted with CsOH to pH 7.2). Seal resistance was typically in the 1–5 GΩ range. Whole cell currents were allowed to stabilize for 2 min before being measured. Immediately after establishment of the whole cell configuration, a protocol consisting of a holding potential of –50 mV for 20 ms followed by a 200 ms linear ramp from –100 mV to +100 mV was performed. This protocol was repeated every 10 s. Capacitive currents and series resistance were determined and corrected using the automatic capacitance and series resistance compensation. All electrophysiological experiments were performed at room temperature.

2.6 Proliferation assay

Cell growth was estimated by determining the cell number. Cells in different groups were seeded at an initial density of 1 × 10^5 cells per well in six-well plates. Cells were harvested and the numbers were counted after 24, 48, 72 and 96 h using a COULTER counter (Beckman, Fullerton, CA, USA). To analyse the effect of TRPC6 on HGF-induced prostate cancer cell proliferation, HGF (20 ng mL^{-1}) was applied 48 h after transfection and the cell numbers were determined 24 h later.

2.7 Cell cycle and cell apoptosis analysis

Cells were trypsinized, harvested and re-suspended in 0.5 mL sterile phosphate-buffered saline (PBS). Cell suspensions were then transferred to 95% ethanol while being mixed thoroughly and stored at room temperature for 30 min. Cells were washed three times with PBS and then treated with ribonuclease (RNase; 100 μg mL^{-1}) for 15 min. Propidium iodide (50 μg mL^{-1}) was added and cells were allowed to incubate for an additional 30 min. Using flow cytometry (Becton Dickinson, San Jose, CA, USA), DNA content was measured by exciting propidium iodide at 488 nm and measuring the emission at 580 nm. The cell cycle stage was then determined and analysed.

Cells were harvested and re-suspended in binding buffer and stained with fluorescein isothiocyanate-coupled annexin V and propidium iodide (Keygen, Nanjing, China). Flow cytometric analysis was performed to quantify the apoptotic cells.

2.8 Intracellular Ca^{2+} measurements

Cells grown on 35 mm glass bottom cell culture dishes were placed in external solution (107 mmol L^{-1} NaCl, 7.2 mmol L^{-1} KCl, 1.2 mmol L^{-1} MgCl$_2$, 2 mmol L^{-1} CaCl$_2$, 11.5 mmol L glucose, 20 mmol L^{-1} HEPES–NaOH [pH 7.2]) and loaded with 5 μmol L^{-1} Fura-2/acetoxymethylester (Fura-2/AM) for 30 min at 37 ºC. Cells were washed, and the dye was allowed to deesterify for a minimum of 30 min at 37 ºC. Fura-2/AM-loaded cells were alternatively excited at 340 and 380 nm, and the emission fluorescence was monitored at 510 nm using a Deltascan spectrofluorometer (Photon Technology International, Lawrenceville, NJ, USA) coupled with a Nikon Diaphot inverted microscope (Nikon, Tokyo, Japan). Fluorescent intensity was recorded over the entire surface of each cell and intracellular Ca^{2+} was evaluated from the ratio of the fluorescent emission intensities produced at the two wavelengths. [Ca^{2+}]$_i$ measurements are shown as the 340/380 nm ratios obtained from groups of single cells (*n* = 6–9). The ratio (R_{exp}) of the

I_f measured during the 340 nm excitation to that during the 380-nm excitation is directly proportional to the $[Ca^{2+}]_i$ in the cells, where $R_{exp} = (I_{f340}-B_{340})/(I_{f380}-B_{380})$. I_{f340} is the I_f measured during excitation at 340 nm; I_{f380} is the I_f measured during excitation at 380 nm; and B_{340} and B_{380} are the background I_f values measured during excitation at 340 and 380 nm, respectively. To allow the experiments to be compared, R_{exp} was normalized (R_{norm}) to the I_{f340}/I_{f380} measured during the *in vitro* calibration in minimal $[Ca^{2+}]_i$ (R_{min}). $R_{norm} = R_{exp}/R_{min}$ [19].

2.9 Statistics

The results are shown as the mean ± SD. Statistical analysis was performed using unpaired *t*-test with the SPSS 12.0 software (SPSS Inc, Chicago, IL, USA), and differences resulting in $P < 0.05$ were considered statistically significant.

3 Results

3.1 The expression of c-MET and TRPC6 in prostate cancer cells

We used RT-PCR to analyse the expression of c-MET and TRPC6 in prostate cancer cells. Figure 1A shows the expression of the transcripts for *TRPC6* and *TRPC6γ* splice variant in DU145, PC3 and 22Rv1 cells, but not in LNCaP cells. We also found the expression of *c-MET* in DU145 and PC3 cells. These results were further confirmed by Western blotting (Figure 1B).

3.2 Gene silencing of TRPC6

The siRNA was used to reduce the expression of TRPC6 in DU145 and PC3 cells. Western blotting showed that the maximal downregulation of the protein occurred 72 h after transfection. At this time, densitometry analysis of Western blots revealed a 70%–80% decrease in TRPC6 protein expression in the TRPC6 siRNA1 (siRNA1) and TRPC6 siRNA2 (siRNA2) groups compared with the TRPC6 siRNA control (siRNAc) and untransfected (control) groups (Figure 2).

3.3 Functional TRPC6 channels are present in DU145 and PC3 cells

Oleoyl-2-acetyl-sn-glycerol (OAG)-induced channel activity in prostate cancer cells was studied using the whole-cell patch clamp technique. To better resolve OAG-activated current in cells, intra- and extracellular solutions were created, which allowed for the elimination of voltage-dependent K^+, replacing K^+ with Cs^+ to
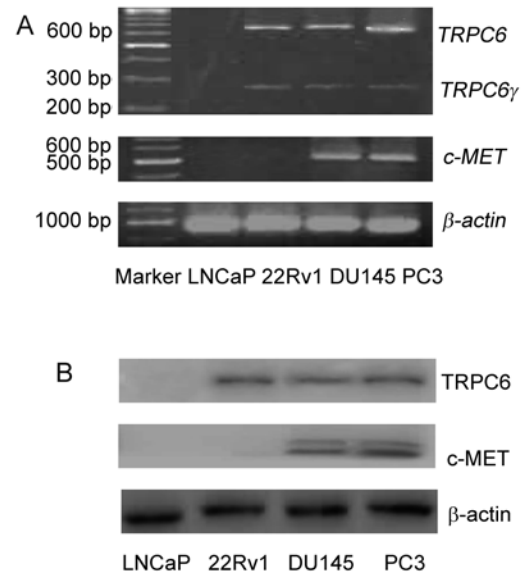

Figure 1. Expression of TRPC6 and c-MET in human prostate cancer cells. (A): RT-PCR detection of *TRPC6* and *c-MET* transcripts in prostate cell lines. The lengths of the *TRPC6*, *TRPC6γ* splice variant and *c-MET* PCR product were 625, 277 and 516 bp, respectively. (B): TRPC6 and c-MET proteins were examined by Western blotting analysis. Equal amounts of cell lysate were separated and immunoblotted with antibodies against TRPC6 and c-MET. TRPC6 was detected in all cell lines except LNCaP. c-MET was detected in DU145 and PC3 cells.

block the K^+ channels. An application of 100 μmol L^{-1} OAG to the bath induced a linear current in the cells. The current/voltage relationship of this OAG-induced current displayed both inward and outward current in DU145 cells (Figure 3B). This current showed a non-selective cation current pattern with a reversal potential close to 0 mV (8.1 ± 1.9 mV). The time course for OAG-induced current at –80 mV revealed an inward current that reached a peak in about 3 min (Figure 3A). Whole-cell clamp patch recordings revealed a substantial decrease in the OAG-induced current after treatment with TRPC6 siRNA1 in DU145 cells. The *I/V* curve showed that both the inward and the outward currents were substantially reduced in the siRNA1 group compared with the control group (Figure 3B). In addition, the OAG-induced peak was greatly diminished (Figure 3A).

The OAG also induced a typical cationic current in PC3 cells. A representative example is shown in Figure 3D. The current that we recorded had a reversal potential of ~ 0 mV (6.4 ± 2.1 mV). The addition of OAG to PC3 cells at a holding potential of –80 mV led to a

The role of TRPC6 in HGF-induced cell proliferation
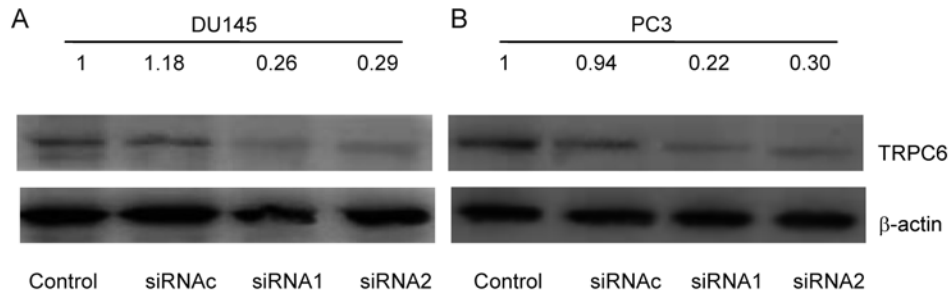Yong Wang *et al*.

npg

845

Figure 2. Transient underexpression of TRPC6. Western blot analysis of total cell lysates isolated from the DU145 (A) or PC3 (B) cells transfected with TRPC6 siRNA1 (siRNA1), TRPC6 siRNA2 (siRNA2) and a siRNA control (siRNAc) for 72 h using the primary anti-TRPC6 antibody. The TRPC6siRNA transfection markedly decreased the level of TRPC6 in DU145 and PC3 cells. The numbers above the gel indicate expression levels with respect to control conditions.
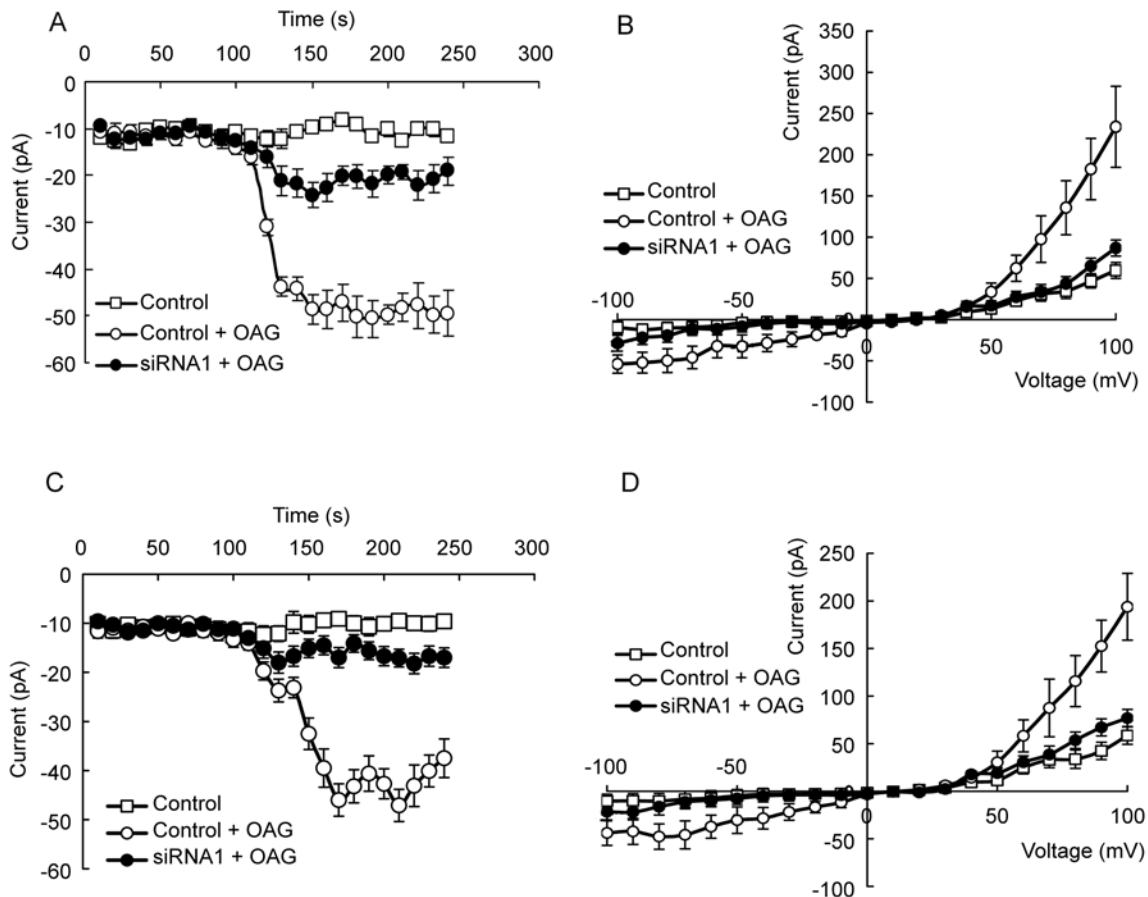

Figure 3. Inhibition of OAG-induced current in DU145 and PC3 cells by TRPC6 siRNA. Averaged time-course development of OAG (100 μmol L^{-1})-induced inward current (measured at –80 mV) in DU145 (A) or PC3 (C) cells. A typical current/voltage (*I/V*) relationship of OAG-induced current in DU145 (B) or PC3 (D) cells recorded at the time of maximum activation determined in A or C. The holding potential was –50 mV for 20 ms and a 200-ms linear ramp from –100 mV to +100mV was applied. The *I/V* curve indicated a double-rectifying property typical for TRPC6, and the reversal potential of the recorded currents was ~0 mV. TRPC6 knockdown inhibited both the outward and the inward current in DU145 and PC3 cells.

current activation that was almost abolished in TRPC6 knockdown cells (Figure 3C). TRPC6 inhibition causes a large reduction in both the outward and the inward currents (Figure 3D).

3.4 Cell proliferation

We examined whether TRPC6 channels affect the growth of DU145 and PC3 cells. The proliferation curves showed no differences in cell proliferation between the siRNAc group and the control group. However, the proliferation of the siRNA1 group was significantly suppressed 48 h after treatment (Figures 4A and C). We then tested whether TRPC6 knockdown affected HGF-induced DU145 and PC3 cell growth. After 48 h of transfection, HGF (20 ng mL^{-1}) was applied, and the cell numbers were determined 24 h later. As shown in Figures 4B and D, TRPC6 knockdown markedly reduced the ability of HGF to increase cell numbers ($P <$ 0.01), indicating that HGF-induced DU145 and PC3 cell proliferation is indeed mediated by TRPC6.

3.5 Cell cycle and apoptosis

To elucidate the mechanism by which TRPC6 inhibition suppresses prostate cancer cell proliferation, we used flow cytometry to examine what effect blocking TRPC6 had on the cell cycle in DU145 and PC3 cells. As showed in Figure 5A and B, the average G$_2$/M percentage of the siRNA1 group (23.29% ± 1.80% and 28.46% ± 2.06% in DU145 and PC3 cells, respectively) was much higher than that of the control group (10.37% ± 1.38% *vs.* 13.54% ± 1.56%, respectively) or the siRNAc group (9.62% ± 1.81% and 15.03% ± 1.63%, respectively) ($P <$ 0.01). This assay suggests that downregulating TRPC6 induces G$_2$/M phase arrest in DU145 and PC3 cells. In Figures 5C and D, the apoptosis ratios in the control, siRNAc and siRNA1 groups of DU145 cells were 3.23% ± 0.69%, 3.54% ± 0.76% and 4.23% ± 0.93%, respectively, indicating that there was no increase in apoptosis after TRPC6 knockdown ($P > 0.05$). Similarly, there were no significant differences in the apoptosis ratio of PC3 cells (control: 4.57% ± 0.71%, siRNAc:
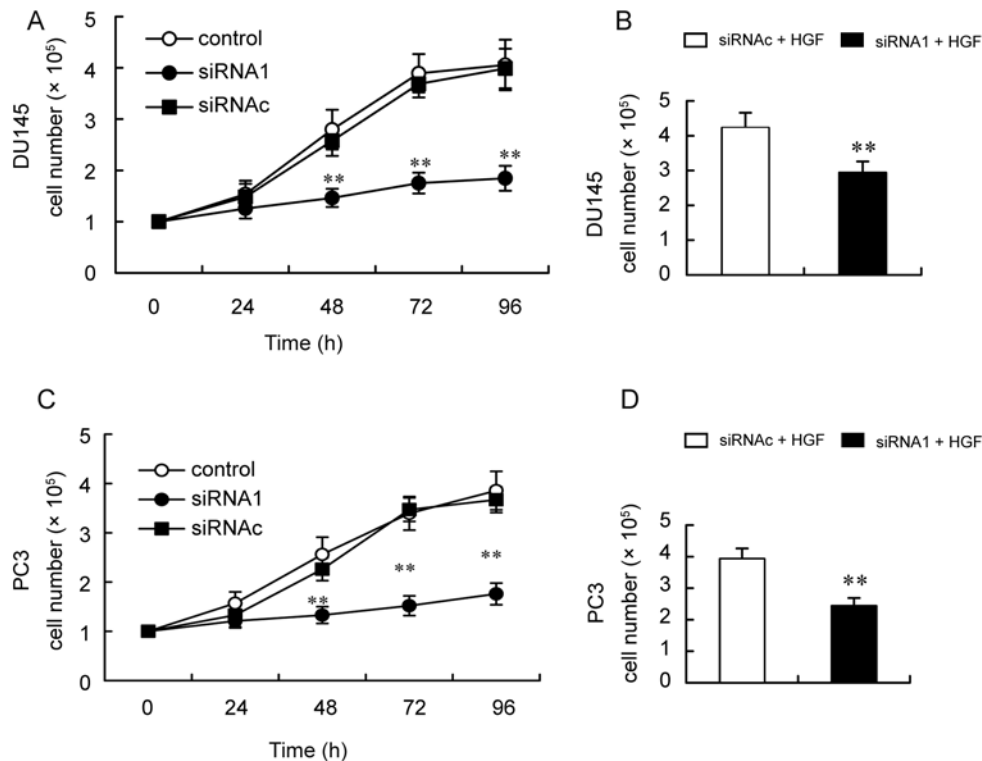

Figure 4. Blocking TRPC6 in DU145 and PC3 cells suppresses cell proliferation. Cell proliferation was evaluated by determining the cell numbers. TRPC6 knockdown inhibited the growth of DU145 (A) or PC3 (C) cells (**$P <$ 0.01 compared with control and siR-NAc). Downregulation of TRPC6 by siRNA abolished HGF-induced proliferation of DU145 (B) and PC3 (D) cells (**$P <$ 0.01 compared with HGF + siRNAc). HGF (20 ng mL^{-1}) was applied 48 h after transfection and the cell numbers were determined 24 h after the application of HGF. Data represent the mean ± SD.

The role of TRPC6 in HGF-induced cell proliferation
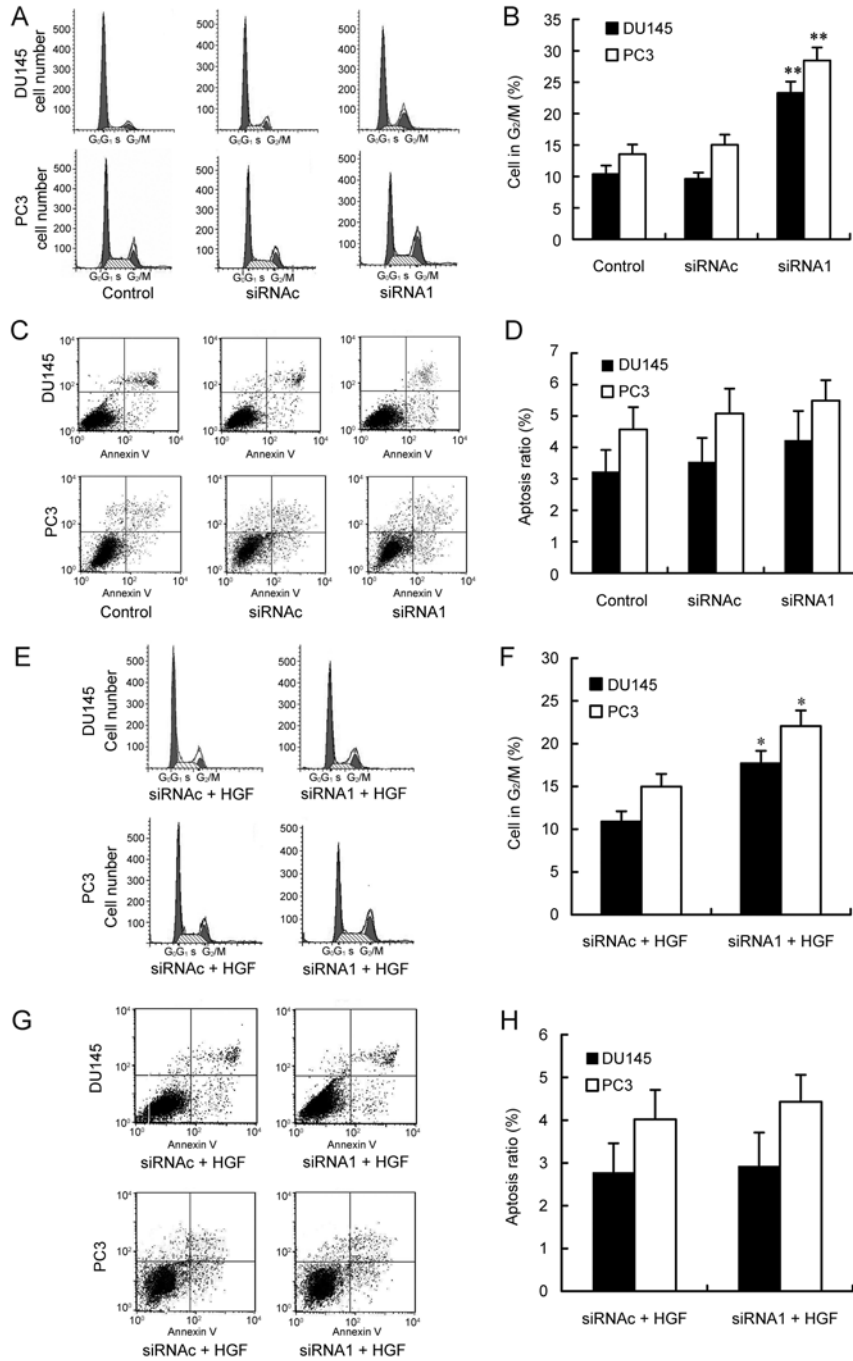Yong Wang *et al*.

npg

847

Figure 5. TRPC6 channels are critical for the G_2/M phase transition in DU145 and PC3 cells. DU145 and PC3 cells were transfected with siRNA1 or siRNAc for 72 h. (A): Cells were fixed, permeabilized and stained with propidium iodide for cell cycle analysis using flow cytometry. (B): Statistics of the percentage of DU145 and PC3 cells in the G_2/M phase. Inhibition of TRPC6-induced G_2/M phase arrest in DU145 and PC3 cells. Data represented the mean ± SD, [**]$P < 0.01$ compared with control and siRNAc. (C), (D): Cells were stained with FITC-coupled Annexin V and propidium iodide. Cell apoptosis percentages were evaluated by flow cytometry. There were no significant differences in the apoptosis ratio between different groups. DU145 and PC3 cells were transfected with siRNA1 or siRNAc for 48 h and then treated with HGF (20 ng mL^{-1}) for an additional 24 h. (E): Flow cytometry of the transfected cells treated with HGF. (F): Statistics of the percentage of cells in G_2/M phase after treatment with HGF. Data represent the mean ± SD, [*]$P < 0.05$ compared with HGF + siRNAc group. (G, H): Cell apoptosis percentages were evaluated by flow cytometry. There were no significant differences in the apoptosis ratio between the different groups.

5.08% ± 0.79% and siRNA1: 5.49% ± 0.65%; $P > 0.05$) (Figures 5C and D).

DU145 and PC3 cells were transfected for 48 h and HGF (20 ng mL^{-1}) was applied for another 24 h. After HGF treatment, the population of cells at the G$_2$/M stage in the HGF + siRNAc group was 10.90% ± 1.19% and 14.97% ± 1.49% in DU145 and PC3 cells, respectively, whereas in the HGF + siRNA1 group, it rose to 17.70% ± 1.46% and 22.06% ± 1.82%, respectively ($P < 0.05$; Figures 5E and F). We also found that the apoptosis ratio was unaffected ($P > 0.05$; Figures 5G and H). In these experiments, the apoptosis ratios did not change in the cells transfected with TRPC6 siRNA1, showing that the reduction in cell number shown in Figure 4 was not due to cell apoptosis. These results suggest that inhibiting TRPC6 induces G$_2$/M phase arrest.

3.6 HGF upregulates TRPC6 expression

A higher plasma level of HGF in prostate cancer patients is associated with an advanced stage of malignancy and a poor prognosis. Therefore, the possible regulation of TRPC6 expression by HGF was investigated. DU145 and PC3 cells were treated for 36 h with 20 ng mL^{-1} of HGF. HGF increased TRPC6 levels in DU145 and PC3 cells (Figure 6).

3.7 TRPC6-mediated calcium entry

We determined the role of TRPC6 in mediating Ca^{2+} entry in DU145 and PC3 cells using Ca^{2+} imaging. Because TRPC6 channels can be activated by diacylglycerol (DAG) [20], we used OAG, a membrane-permeable analogue of DAG, to test Ca^{2+} inflow in cells.
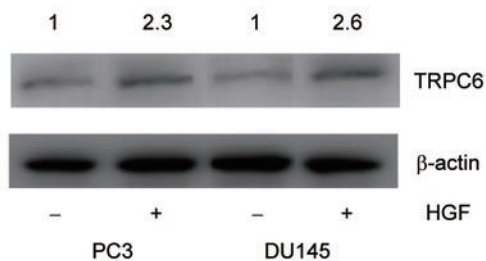

Figure 6. TRPC6 expression and HGF. Western blotting showed an increase in TRPC6 levels in DU145 and PC3 cells in the presence of HGF (20 ng mL^{-1}) for 36 h. +HGF (20 ng mL^{-1}), −: HGF (0) (control). The band densities are shown as ratios: objective band density/β-actin density. The band density of the control group was normalized to 1 and the numbers above the gels indicate expression levels with respect to control conditions.

The data show that OAG increased [Ca^{2+}]$_i$ (Figure 7A). The increased [Ca^{2+}]$_i$ was due to entry, as there was no OAG-induced [Ca^{2+}]$_i$ increase in the absence of extracellular Ca^{2+}. A further experiment examined the effects of TRPC6 knockdown on Ca^{2+} entry. As indicated in Figure 7A, OAG-induced Ca^{2+} entry obviously decreased in the siRNA1 group compared with the siRNAc and control groups. We then investigated the change in OAG-induced Ca^{2+} entry in DU145 cells after treatment with HGF for 36 h and found a large increase in OAG-induced Ca^{2+} entry (Figure 7A). Hence, TRPC6 overexpression in HGF-treated DU145 cells is expected to lead to an increase in [Ca^{2+}]$_i$.

To address whether HGF can activate TRPC6 in DU145 cells, DU145 cells were transfected with siRNA1 or siRNAc. HGF (20 ng mL^{-1}) resulted in a significant increase in [Ca^{2+}]$_i$ after 6 min of incubation in the siRNAc group, whereas [Ca^{2+}]$_i$ only slightly increased in the siRNA1 group (Figure 8A).

As shown by Fura-2/AM imaging, OAG- and HGF-induced calcium influx could also be recorded in PC3 cells. The elevation in [Ca^{2+}]$_i$ induced by OAG is due to an influx of extracellular Ca^{2+} in PC3 cells. Moreover, the [Ca^{2+}]$_i$ elevation induced by OAG and HGF was attenuated when TRPC6 was inhibited in PC3 cells (Figures 7B and 8B).

4 Discussion

To find possible effectors of the biological outcome of HGF, we focused on TRPC6 cation channels, because cation channels have a part in the regulation of cellular functions (proliferation and migration, for example) that are typically induced by HGF. In this study, we found the following: (1) TRPC6 and c-MET were expressed in DU145 and PC3 cells; (2) TRPC6 channels could regulate the non-voltage-dependent cation currents in DU145 and PC3 cells; (3) knockdown of TRPC6 channels in DU145 and PC3 cells suppressed HGF-induced cell proliferation and arrested the cell cycle at the G$_2$/M phase; (4) HGF increased TRPC6 expression; and (5) the HGF-induced increase in intracellular calcium was mediated by TRPC6 in DU145 and PC3 cells. These results suggest that the TRPC6 channel-regulated Ca^{2+} inflow is essential for the HGF-induced cell proliferation of DU145 and PC3 human prostate cancer cells.

In this study, TRPC6 was undetectable in LNCaP cells. This result is in line with studies by Thebault
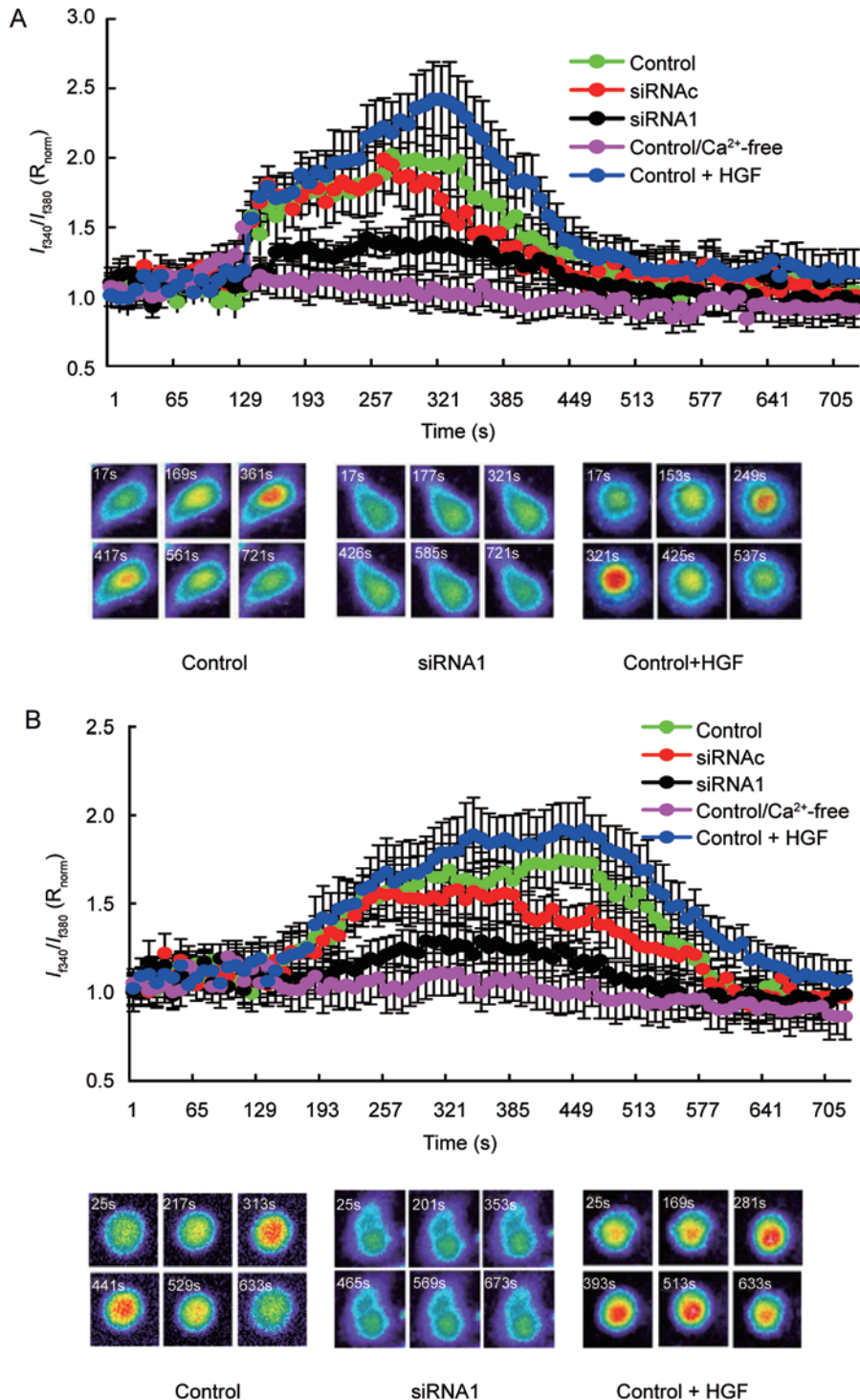
The role of TRPC6 in HGF-induced cell proliferation
Yong Wang *et al*.

npg

849

Figure 7. OAG-induced Ca^{2+} entry is mediated by TRPC6. DU145 and PC3 cells were transfected with siRNA1 or siRNAc or treated with 20 ng mL^{-1} of HGF for 36 h. Cells were then loaded with Fura-2/AM, and the OAG-induced Ca^{2+} entry was estimated from the fluorescent intensity. (A, B) Time courses (the upper panels) and representative fluorescence microscopy images (lower panels, taken at one frame per 8 s; the time is indicated in the images) of 100 μmol L^{-1} OAG-induced Ca^{2+} entry in DU145 (A) and PC3 (B) cells in the absence or presence of 2 mmol L^{-1} extracellular Ca^{2+}. These results suggest that the activation of TRPC6 channels is indeed involved in OAG-induced Ca^{2+} entry in DU145 and PC3 cells. Data represent the mean ± SD.

The role of TRPC6 in HGF-induced cell proliferation
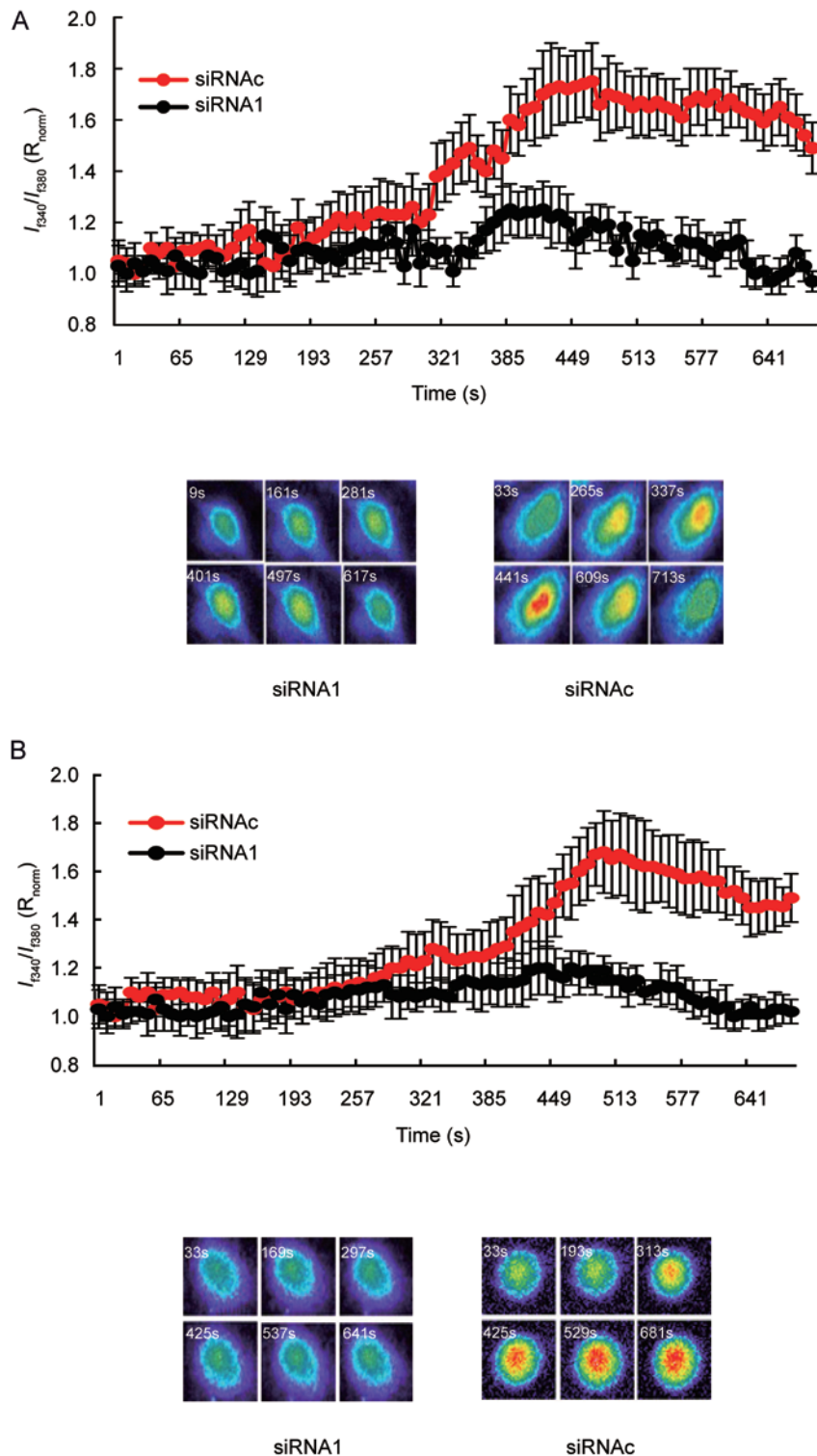Yong Wang *et al*.

850

Figure 8. HGF-increased intracellular calcium is mediated by TRPC6. DU145 and PC3 cells were transfected with either siRNA1 or siRNAc, loaded with Fura-2/AM and then treated with 20 ng mL^{-1} HGF. (A, B): Time courses (the upper panels) and representative fluorescence microscopy images (lower panels, taken at one frame per 8 s; the time is indicated in the images) of 20 ng mL^{-1} of HGF-induced Ca^{2+} influx in DU145 (A) and PC3 (B) cells in the presence of 2 mmol L^{-1} extracellular Ca^{2+}. The HGF-induced increase in intracellular calcium is mediated by TRPC6 in DU145 and PC3 cells. Data represent the mean ± SD.

et al. [11]. The HGF receptor, c-MET, was detected in DU145 and PC3 cells but not in LNCaP and 22Rv1 cells in our study. It has been observed that c-MET expression is inversely correlated with the expression of the androgen receptor [21, 22]. Moreover, c-MET-protein is frequently detected in high-grade prostate cancers and metastatic tumour samples [22, 23]. Thus, our work and several lines of experimental evidence presented here support an association of c-MET expression with two indicators of prostatic tumour progression: metastasis and androgen insensitivity. Similar to other research [24], we found that OAG-activated cationic channels in cells had certain electrophysiological properties (inward and outward currents and voltage independence). This current displayed a non-selective cation current pattern with a reversal potential close to 0 mV. Knocking down TRPC6 reduced both inward and outward currents. These results suggest that there are indeed functional TRPC6 channels in DU145 and PC3 cells. Overall, our data suggest that DU145 and PC3 cells offer a useful system to study the relationship between endogenous TRPC6 channels and HGF in prostate cancer.

Our results indicate that HGF and the DAG analogue, OAG, activate Ca^{2+} entry mainly through TRPC6 channels. Cytosolic Ca^{2+} is an important transducer of HGF signals. The mechanisms through which HGF-induced calcium entry occurs are still controversial. The activation of c-MET by HGF causes the sustained formation of DAG and inositol 1,4,5 triphosphate (IP_3) by PLC [25]. These observations fit well with TRPC6 mediating the HGF-induced inflow of extracellular Ca^{2+}. TRPC6 channels function as store-operated calcium channels that account for the sustained calcium inflow triggered by the IP_3-evoked depletion of intracellular Ca^{2+} stores [9]. Furthermore, TRPC6, as a receptor-operated Ca^{2+} channel in primary hPCE cells, is also directly activated by DAG [11, 12]. Although it is not clear whether HGF can induce Ca^{2+} entry independent of store depletion in DU145 cells, our results suggest that TRPC6 is instrumental to HGF-induced calcium entry in DU145 and PC3 cells.

The Ca^{2+} signalling is critical for cell proliferation [3]. Oscillatory $[Ca^{2+}]_i$ activity may be especially suited to the specificity of Ca^{2+} signalling [26], as the possibility of amplitude and frequency signal encoding permits distinct effectors to be targeted. Recent data suggested that Ca^{2+} entry through TRPC6 enhances primary hPCE cell proliferation [12]. In our study, we not only uncover the involvement of TRPC6 in HGF-

induced Ca^{2+} entry in DU145 and PC3 cells but also show the likely role of this channel in the enhancement of the proliferative effects of HGF, because exposure to HGF causes TRPC6 overexpression. Thus, remodelling the expression and activity of TRPC6 may account for two mechanisms involved in HGF-induced prostate cancer cell proliferation. Another important finding of the present study is that TRPC6 affects cell proliferation without addition of HGF. Thus, activation of TRPC6 is sufficient to stimulate cell proliferation. It is not clear how TRPC6 is activated under basal conditions in our cultures. It is possible that growth factors, such as VEGF [19] and EGF [9], in the culture medium during basal conditions activate TRPC6. Inconsistent with our results, some research has indicated that overexpressing wild-type TRPC6 in some types of cancer cells does not enhance cell proliferation [10, 27]. We suggest that the difference between endogenous and exogenous expression causes the different effects.

Our study supports that TRPC6 is critical for the G_2/M phase transition [10, 27], whereas TRPM8 is important for the G1/S phase transition in PC3 cells [28]. It is thus possible that the distinct effects of these channels on the cell cycle may be due to their actions on different downstream effectors that affect the cell cycle. Ca^{2+} signalling checkpoints are important for cancer cell cycle processes, which are critical for cell proliferation [3]. Indeed, the G_2/M phase transition is critical for maintaining genomic stability [29]. High levels of TRPC6 expression might affect the G_2/M phase transition and eventually contribute to genomic instability in prostate cells, which could result in prostate cells accumulating favourable mutations and becoming more malignant. Therefore, the $[Ca^{2+}]_i$ regulated by TRPC6 affects the G_2/M phase transition and proliferation of DU145 and PC3 cells.

TRPC6 is expressed in DU145 and PC3 cells, but not in LNCaP cells. However, Ca^{2+} entry in the three cell types can be induced by OAG [11]. A homo- or heterotetrameric assembly of TRPC probably forms the endogenous DAG-gated cationic channel in prostate cancer cells. It is not entirely clear whether TRPC6 by itself or by forming homo- or heterotetramers with other members of TRPC (for example TRPC3) is involved in the development of DU145 and PC3 cells. Therefore, further studies are needed to examine the effects of TRPC coexpression and TRPC interactions in prostate cancer.

Our results show that TRPC6 is expressed and

functional in DU145 and PC3 human prostate cancer cells. Moreover, TRPC6-regulated $[Ca^{2+}]_i$ elevation controls the G_2/M phase transition, thus affecting HGF-induced proliferation of prostate cancers. Combined with our previous study, our findings strongly indicate that blocking the HGF-stimulated intracellular signalling pathway, both at the receptor level and at the level of the affected ion channel, might be used to treat prostate cancer.

References

1   Feldman BJ, Feldman D. The development of androgen-independent prostate cancer. Nat Rev Cancer 2001; 1: 34–45.

2   Pardo LA, Stühmer W. Eag1: an emerging oncological target. Cancer Res 2008; 68: 1611–3.

3   Roderick HL, Cook SJ. Ca^{2+} signalling checkpoints in cancer: remodelling Ca^{2+} for cancer cell proliferation and survival. Nat Rev Cancer 2008; 8: 361–75.

4   Kahl CR, Means AR. Regulation of cell cycle progression by calcium/calmodulin-dependent pathways. Endocr Rev 2003; 24: 719–36.

5   Vanoverberghe K, Vanden Abeele F, Mariot P, Lepage G, Roudbaraki M, *et al.* Ca^{2+} homeostasis and apoptotic resistance of neuroendocrine-differentiated prostate cancer cells. Cell Death Differ 2004; 11: 321–30.

6   Hardie RC, Minke B. The *trp* gene is essential for a light-activated Ca^{2+} channel in Drosophila photoreceptors. Neuron 1992; 8: 643–51.

7   Ramsey IS, Delling M, Clapham DE. An introduction to TRP channels. Annu Rev Physiol 2006; 68: 619–47.

8   Guilbert A, Dhennin-Duthille I, Hiani YE, Haren N, Khorsi H, *et al.* Expression of TRPC6 channels in human epithelial breast cancer cells. BMC Cancer 2008; 8: 125.

9   El Boustany C, Bidaux G, Enfissi A, Delcourt P, Prevarskaya N, *et al.* Capacitative calcium entry and transient receptor potential canonical 6 expression control human hepatoma cell proliferation. Hepatology 2008; 47: 2068–77.

10   Cai R, Ding X, Zhou K, Shi Y, Ge R, *et al.* Blockade of TRPC6 channels induced G2/M phase arrest and suppressed growth in human gastric cancer cells. Int J Cancer 2009; 125: 2281–7.

11   Thebault S, Roudbaraki M, Sydorenko V, Shuba Y, Lemonnier L, *et al.* Alpha1- adrenergic receptors activate Ca^{2+}-permeable cationic channels in prostate cancer epithelial cells. J Clin Invest 2003; 111: 1691–701.

12   Thebault S, Flourakis M, Vanoverberghe K, Vandermoere F, Roudbaraki M, *et al.* Differential role of transient receptor potential channels in Ca^{2+} entry and proliferation of prostate cancer epithelial cells. Cancer Res 2006; 66:2038–47.

13   Hashem M, Essam T. Hepatocyte growth factor as a tumor marker in the serum of patients with prostate cancer. J Egypt Natl Canc Inst 2005; 17: 114–20.

14   Yasuda K, Nagakawa O, Akashi T, Fujiuchi Y, Koizumi K, *et al.* Serum active hepatocyte growth factor (AHGF) in benign prostatic disease and prostate cancer. Prostate 2009; 69: 346–51.

15   Kawanishi T, Kato T, Asoh H, Uneyama C, Toyoda K, *et al.* Hepatocyte growth factor-induced calcium waves in hepatocytes as revealed with rapid scanning confocal microscopy. Cell Calcium 1995; 18: 495–504.

16   Rampino T, Gregorini M, Guidetti C, Broggini M, Marchini S, *et al.* KCNA1 and TRPC6 ion channels and NHE1 exchanger operate the biological outcome of HGF/scatter factor in renal tubular cells. Growth Factors 2007; 25: 382–91.

17   Yue D, Wang Y, Xiao JY, Wang P, Ren CS. Expression of TRPC6 in benign and malignant human prostate tissues. Asian J Androl 2009; 11: 541–7.

18   Yue D, Wang Y, Ma P, Li YY, Chen H, *et al.* Effects of transferred NK4 gene on proliferation, migration, invasion and apoptosis of human prostate cancer DU145 cells. Asian J Androl 2010; 12: 381–9.

19   Hamdollah Zadeh MA, Glass CA, Magnussen A, Hancox JC, Bates DO. VEGF-mediated elevated intracellular calcium and angiogenesis in human microvascular endothelial cells in vitro are inhibited by dominant negative TRPC6. Microcirculation 2008; 15: 605–14.

20   Hofmann T, Obukhov AG, Schaefer M, Harteneck C, Gudermann T, *et al.* Direct activation of human TRPC6 and TRPC3 channels by diacylglycerol. Nature 1999; 397: 259–63.

21   Humphrey PA, Zhu X, Zarnegar R, Sw=anson PE, Ratliff TL, *et al.* Hepatocyte growth factor and its receptor (c-MET) in prostatic carcinoma. Am J Pathol 1995; 147(2): 386–96.

22   Knudsen BS, Gmyrek GA, Inra J, Scherr DS, Vaughan ED, *et al.* High expression of the Met receptor in prostate cancer metastasis to bone. Urology 2002; 60: 1113–7.

23   Pisters LL, Troncoso P, Zhau HE, Li W, von Eschenbach AC, *et al.* c-Met proto-oncogene expression in benign and malignant human prostate tissues. J Urol 1995; 154: 293–8.

24   Clapham DE. TRP channels as cellular sensors. Nature 2003; 426: 517–24.

25   Osada S, Nakashima S, Saji S, Nakamura T, Nozawa Y. Hepatocyte growth factor (HGF) mediates the sustained formation of 1, 2-diacylglycerol via phosphatidylcholine -phospholipase C in cultured rat hepatocytes. FEBS Lett 1992; 297: 271–4.

26   Dolmetsch RE, Xu K, Lewis RS. Calcium oscillations increase the efficiency and specificity of gene expression. Nature 1998; 392: 933–6.

27   Shi Y, Ding X, He ZH, Zhou KC, Wang Q, *et al.* Critical role of TRPC6 channels in G_2 phase transition and the development of human oesophageal cancer. Gut 2009; 58: 1443–50.

28   Yang ZH, Wang XH, Wang HP, Hu LQ. Effects of TRPM8 on the proliferation and motility of prostate cancer PC-3 cells. Asian J Androl 2009; 11: 157–65.

29   Sancar A, Lindsey-Boltz LA, Unsal-Kacmaz K, Linn S. Molecular mechanisms of mammalian DNA repair and the DNA damage checkpoints. Annu Rev Biochem 2004; 73: 39–85.